

# Millimeter and submillimeter spectroscopy of methylallene, $\text{CH}_3\text{CHCCH}_2$

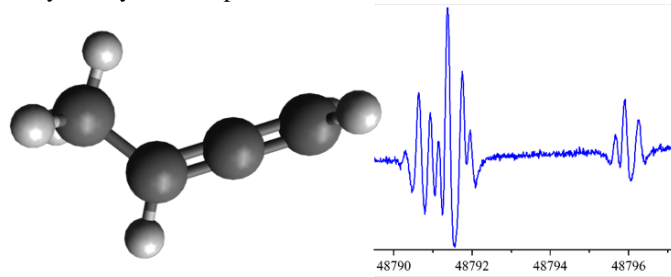
Holger S. P. Müller<sup>a,\*</sup>, Frank Lewen<sup>a</sup>, Jean-Claude Guillemin<sup>b</sup>, Stephan Schlemmer<sup>a</sup>

<sup>a</sup>*I. Physikalisches Institut, Universität zu Köln, Zülpicher Str. 77, 50937 Köln, Germany*

<sup>b</sup>*Univ Rennes, Ecole Nationale Supérieure de Chimie de Rennes, CNRS, ISCR-UMR 6226, 35000 Rennes, France*

## Abstract

Small polycyclic aromatic hydrocarbons and somewhat larger cyano derivatives were detected in the cold dark cloud TMC-1 recently. Their formation from smaller hydrocarbons is not well understood, in part because abundances of many species are not known. Methylallene,  $\text{CH}_3\text{CHCCH}_2$ , may be one of the building blocks, but its rotational spectrum was characterized only to a very limited extent. We recorded rotational transitions in the 36–501 GHz region to extend the existing line list of methylallene and thus enable searches for the molecule in space. Quantum-chemical calculations were carried out to evaluate initial spectroscopic parameters. We obtained transition frequencies with  $J \leq 61$  and  $K_a \leq 21$  and resolved the internal rotation splitting of the  $\text{CH}_3$  group at least partially. As a result, a full set of distortion parameters up to sixth order along with two octic ones were determined, as well as parameters describing the internal rotation of the methyl group. The spectroscopic parameters are accurate enough to identify methylallene up to 720 GHz, sufficient for searches even in the warm interstellar medium.



## Keywords:

rotational spectroscopy, internal rotation, interstellar molecule, hydrocarbon

## 1. Introduction

More than 340 different molecules have been detected in the interstellar medium (ISM) and in circumstellar shells of late-type stars thus far, see the Molecules in Space webpage [1] of the Cologne Database for Molecular Spectroscopy, CDMS [2, 3], for an up-to-date list. A substantial fraction of the recent detections was made in the cold and dark molecular cloud TMC-1. They include the polycyclic aromatic hydrocarbon (PAH) molecules indene [4, 5] and phenalene [6] along with several PAH cyano derivatives up to cyanocoronene [7], a molecule containing seven fused benzene rings. The abundances were interpreted in favor of a formation of these molecules in TMC-1 from smaller hydrocarbons (bottom-up chemistry) rather than from a break-up of even larger molecules (top-down chemistry) [8]. Several small to moderately sized hydrocarbons were detected in space, in earlier years often very unsaturated ones with more C than H atoms, in part because they often have substantial dipole moments. More saturated hydrocarbons usually have small or even zero dipole moments,

making it difficult or impossible to detect them by means of radio astronomy. However, chemical aspects are very important also. Unsaturated molecules, often very unsaturated ones, are very abundant in cold dark molecular clouds whereas (fairly) saturated molecules dominate in the warm parts of star-forming regions. There is a fairly common misconception that abundances of molecules in space would be governed by their relative energies. For example among the  $\text{C}_3\text{H}_4\text{O}$  isomers, propadienone ( $\text{H}_2\text{CCCO}$ ) has been elusive until very recently [9] even though it is lower in energy than propynal and much lower than cyclopropenone. Shingledecker et al. [10] showed that the reaction between propadienone and atomic hydrogen is barrierless, making it difficult to accumulate propadienone in space. But kinetics does not only govern astrochemistry, it is also dominant under more ambient conditions. For example the primary products in the reaction of Cl atoms with  $\text{NO}_2$  at room temperature with an excess of  $\text{N}_2$  are  $\text{ClONO}$  and  $\text{ClNO}_2$  with  $\text{ClONO}$  initially four times as abundant as  $\text{ClNO}_2$  despite the latter being  $\sim 10$  kcal/mol lower in energy [11].

Propene,  $\text{C}_3\text{H}_6$ , also known as (aka) propylene, was detected nearly 20 years ago in TMC-1 [12], was later found in several other cold clouds [13, 14], and was even found in the luke-

\*Corresponding author.

Email address: [hspm@ph1.uni-koeln.de](mailto:hspm@ph1.uni-koeln.de) (Holger S. P. Müller)

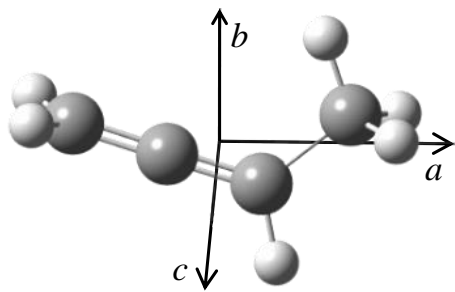


Figure 1: Sketch of the methylallene molecule. Carbon atoms are symbolized by gray spheres while hydrogen atoms are indicated by small, light gray spheres. The *a*-axis is in the paper plane and the *b*-axis is rotated slightly toward the viewer.

warm parts surrounding the low-mass protostar IRAS 16292-2422B [15]. More recently, isobutene,  $(\text{CH}_3)_2\text{CCH}_2$ , was identified in the cold and presumably shocked molecular cloud G+0.693-0.027 [14] in the vicinity of the high-mass star forming region Sagittarius B2(N) close to the Galactic center, and 1-butyne,  $\text{C}_2\text{H}_5\text{CCH}$ , aka ethylacetylene, was found unambiguously soon thereafter in TMC-1 [16].

Methylallene (Figure 1),  $\text{CH}_3\text{CHCCH}_2$ , aka 1,2-butadiene, is an isomer of 1- and 2-butyne and also of 1,3-butadiene. The low-energy *trans*-1,3-butadiene conformer has no permanent dipole moment, such that methylallene may serve as a proxy for the former and possibly also for allene,  $\text{H}_2\text{CCCH}_2$ , which also has no permanent dipole moment. It should be pointed out that there is a *gauche* conformer of 1,3-butadiene with a very small dipole moment, which was characterized by rotational spectroscopy [17], but it is 2.93 kcal/mol (1475 K) higher in energy [18]. While 1,3-butadiene was thought to be an important molecule for the formation of at least some PAH molecules, this role was questioned in a recent rebuttal of the detection of 1-cyano-1,3-butadiene, aka 2,4-pentadienenitrile [19]. It appears plausible that methylallene can act as an additional building block for larger hydrocarbons, even more so, as the related ethynylallene, aka allenylacetylene or 1,2-pentadien-4-yne is among the fairly unsaturated molecules detected in space [20].

The rotational spectrum of methylallene was studied almost 70 years ago in the microwave region by Lide and Mann [21] with observations of splittings, caused by the hindered internal rotation of the methyl group, often resolved and with the determination of dipole moment components. A marginal extension of the spectrum to  $\sim$ 50 GHz was reported by Ogata [22] in the course of a structure determination of methylallene.

We studied the rotational spectrum of methylallene extensively up to submillimeter wavelengths in order to be able to elucidate its importance in astrochemistry. The resulting spectroscopic parameters are deemed to be accurate enough to search for methylallene not only in cold and dark molecular clouds, but also in the warmer parts of star-forming regions because of the accurately measured higher frequency transitions.

## 2. Experimental details

### 2.1. Sample preparation

The original synthesis [23] was reproduced with some minor modifications in the final step: the reflux condenser was maintained at 20–25°C, and nitrogen was used instead of carbon dioxide for bubbling. The crude product thus obtained was purified by trap-to-trap distillation under vacuum (0.1 mbar). The high-boiling compounds were condensed in the first trap, immersed in a cooling bath at  $-100^\circ\text{C}$ , while methylallene was selectively condensed in the second trap, immersed in a liquid nitrogen bath. This purification was repeated once. A yield of 68% was determined by weighing the trapped compound and by  $^1\text{H}$  NMR analysis, which revealed the presence of 1–2% ethanol.

### 2.2. Spectroscopic measurements

Measurements at the Universität zu Köln were carried out between 36 and 501 GHz applying two slightly different spectrometer setups. One is equipped with two connected 7 m long glass cells in a single path arrangement sealed with Teflon windows and with different Schottky diode detectors. An Agilent E8257D synthesizer at fundamental frequencies was used as source for measurements between 35 and 69 GHz, while this synthesizer together with a VDI frequency tripler was employed between 71 and 117 GHz. Employing a frequency multiplier from RPG instead of the VDI frequency tripler enabled measurements between 143 and 165 GHz. The sample pressure was between 2.0 and 3.0 Pa, and the frequency modulation was chosen so that the intensities of stronger lines were slightly below their maximum. This setup is similar to the one employed by Ordu et al. [24].

A combination of an active and passive frequency multipliers from the VDI starter kit driven by a Rohde & Schwarz SMF 100A synthesizer was used for spectral recordings in the 344 to 501 GHz region. A 5 m long double path cell was equipped with a Teflon window and a retro reflector which rotated the polarisation by 90°. A Schottky diode was employed as detector. The spectrometer was described in detail earlier [25].

In order to achieve narrow lines, the modulation was lowered for these measurements to the point at which the line-width decrease was still more pronounced than the loss in intensity. The sample pressure could be raised to between 5.0 and 7.0 Pa without substantial increase in line-width. Frequency modulation was applied throughout; the demodulation at  $2f$  causes the lines to appear close to the second derivative of a Gaussian. As the rotational spectrum of methylallene is fairly weak even for the strongest lines, only individual transitions or small groups thereof were recorded with integration times adjusted to reach good signal-to-noise ratios.

## 3. Quantum-chemical calculation

We carried out quantum-chemical calculations at the Regionales Rechenzentrum der Universität zu Köln (RRZK) using

the commercially available program Gaussian 16 [26]. We performed B3LYP hybrid density functional calculations [27, 28] employing the correlation consistent basis set augmented with diffuse basis functions aug-cc-pVTZ [29], the basis set is abbreviated here to 3a, and the entire model is described as B3LYP/3a. An equilibrium geometry was determined by analytic gradient techniques, the harmonic force field by analytic second derivatives, and the anharmonic force field by numerical differentiation of the analytically evaluated second derivatives of the energy. The main goal of the anharmonic force field calculation was the determination of ground state rotational parameters along with equilibrium quartic and sextic centrifugal distortion parameters.

#### 4. Spectroscopic properties of methylallene and previous investigations

Methylallene is an asymmetric rotor of the prolate type with  $\kappa = (2B - A - C)/(A - C)$  being with  $-0.9818$  quite close to the limiting case of  $-1$ . A model of the molecule is shown in Figure 1. The molecule possesses a fairly small  $a$ -dipole moment component of  $0.397$  D and an even smaller  $b$ -component of  $0.071$  D. Please note that these values differ from the reported  $0.394 \pm 0.002$  D and  $0.070 \pm 0.001$  D [21] because a value of  $0.709$  D was applied for the OCS reference whereas the current best value is  $0.71519$  D [30, 31]. The strongest  $a$ -type transitions,  $R$ -branch transitions having  $J' - J'' = +1$ , are about a factor of 20 stronger near  $40$  GHz than the strongest  $b$ -type transitions, which are  $K_a = 1 - 0$   $Q$ -branch ( $J' - J'' = 0$ ) transitions. Other  $b$ -type transitions as well as  $a$ -type  $Q$ -branch transitions are weaker still.

Lide and Mann studied the microwave spectrum of methylallene between  $15.9$  and  $33.1$  GHz and recorded the  $J = 2 - 1$  to  $4 - 3$   $a$ -type rotational transitions [21]. They resolved in many cases the splitting caused by the hindered internal rotation of the  $\text{CH}_3$  group which amounted to a few megahertz in the most favorable cases. They derived a barrier height  $V_3$  to internal rotation of  $556 \pm 2$   $\text{cm}^{-1}$  ( $800$  K). The splitting between the totally symmetry A component and the doubly degenerate E component in the  $a$ -type  $R$ -branch transitions is usually less than  $\sim 3$  MHz, whereas it is up to  $\sim 50$  MHz for  $b$ -type and for  $a$ -type  $Q$ -branch transitions.

In cases in which the asymmetry splitting of a pair of rotational energies with the same  $J$  and the same  $K_a$  is close to the splitting between the A and E levels, mixing may occur between the E components. This mixing causes the energy levels to repel each other and results in larger A/E splittings particularly noteworthy in the  $a$ -type  $R$ -branch transitions. An additional effect of the mixing between the two levels is that usually forbidden  $x$ -type ( $\Delta K_a$  and  $\Delta K_c$  are  $0 \bmod 2$ ) or  $c$ -type ( $\Delta K_a = 1 \bmod 2$  and  $\Delta K_c = 0 \bmod 2$ ) transitions borrow some intensity from the strongly allowed transitions. The spin-statistics of the  $\text{CH}_3$  group are such that the A and E components of a given transition have the same intensities in the absence of such interactions.

In a study of several methylallene isotopologs in order to determine structural parameters of the molecule, Ogata deter-

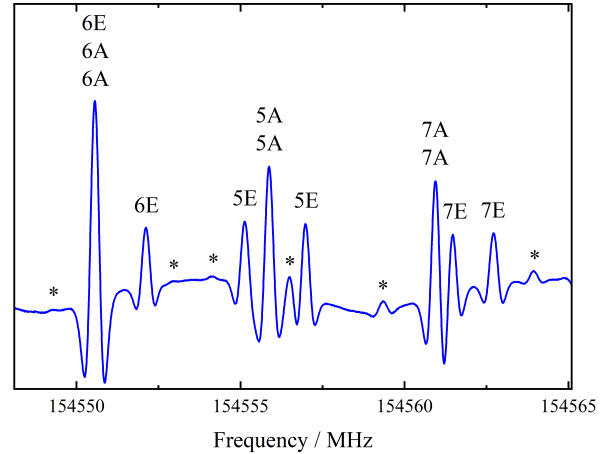


Figure 2: Section of the millimeter wave spectrum of methylallene in the region of the  $J = 19 - 18$  higher  $K_a$   $a$ -type transitions. The  $K_a$  quantum numbers as well as the methyl internal rotor symmetry labels A and E are indicated. The asymmetry splitting of the two transitions in each higher  $K_a$  is unresolved in the A components, while the E components occur in different locations. Several unassigned lines, indicated by asterisks, probably originate from excited vibrational states of methylallene.

mined  $J = 6 - 5$  A symmetry transition frequencies of the main species around  $48$  GHz, but these were soon replaced by present, more accurate measurements [22].

#### 5. Spectroscopic results

The rotational spectrum of methylallene was fit and calculated with the Erham program [32, 33]. The low-order parameters describing the internal rotation are  $\rho$ ,  $\beta$ , and  $\epsilon$ , which represent the length of the  $\rho$ -vector, its angle with the  $a$ -axis, and the first order tunneling parameter, respectively. Strictly speaking,  $\epsilon$  should read  $\epsilon_1$ , but since we do not utilize any higher order tunneling parameters, we omitted the subscript. Furthermore, we prefer shorter notations  $\epsilon_K$ ,  $\epsilon_J$ ,  $\epsilon_2$ , etc. for  $[A - (B + C)/2]$ ,  $[(B+C)/2]$ ,  $[(B-C)/4]$ , etc., respectively, with one reason being that these notations are more common in other programs.

As the previous line list was very limited, quartic centrifugal distortion parameters from a quantum-chemical calculation described in Sect. 3 were included into the parameter set and only released if this resulted in a sufficient improvement of the weighted rms.

In the first measurement rounds,  $a$ -type  $R$ -branch transitions were recorded in the  $36 - 69$  GHz region. As can be seen in Figure 2 for somewhat higher frequencies, the internal rotation patterns of transitions with higher  $K_a$  are distinct. The asymmetry splitting between the A components is often unresolved, and the E components may occur on either side or may sometimes be blended with the two A components, as in the case of  $K_a = 6$  in Figure 2. There are also several unassigned lines in that figure which are likely caused by vibrational satellites, which sometimes affect the positions of the  $a$ -type  $R$ -branch transitions. Interestingly, it appeared as if  $b$ -type lines were less affected by blending in spite of their lower intensities as long as they were not close to frequency regions with  $a$ -type  $R$ -branch

transitions. These measurements of  $a$ -type  $R$ -branch transitions constrained  $B$ ,  $C$ ,  $D_J$ ,  $D_{JK}$  and  $d_1$  quite well along with  $\rho$ ,  $\beta$ , and  $\epsilon$ . Even  $A$  was quite well constrained with an uncertainty of 0.63 MHz after 150 MHz initially [21] and 25 MHz later [22]. Therefore, we searched for the relatively strong  ${}^rQ_0$   $b$ -type transitions. The superscript indicated the change from  $K''_a$  to  $K'_a$ , and the subscript indicates that  $K''_a$  is 0. The E symmetry components were found well within the uncertainties while the A symmetry components appeared just within uncertainties.

Subsequently, further  $b$ -type transitions were recorded, first in the 36–69 GHz region and later in the 71–117 GHz and 143–165 GHz regions. These covered  ${}^pR_1$  and  ${}^rR_0$  transitions and went in  $K_a$  up to the  ${}^rP_5$  and  ${}^rP_6$  transitions, extending to  $J = 64$  and  $K_a = 7$ . Generally, we tried to record as many transitions belonging to a particular series as possible with reasonable integration times. In order to constrain the asymmetry splitting and the internal rotation parameters further,  $a$ -type  $Q$ -branch transitions with  $K_a = 1$  to 3 were recorded.

In all frequency regions, including the 344–501 GHz region, we recorded  $a$ -type  $R$ -branch transitions. We reached the  $K_a = J''$  levels up to  $J'' = 17$ , covering  $J'' = 4$  to 13 and 17 to 19, while we accessed  $K_a$  up to 21 in the submillimeter region. Extrapolation of the Hamiltonian model into the highest frequency region was very good, in particular for transitions with relatively low  $J$  ( $\lesssim 50$ ) and  $K_a$  up to about 10 because the  $b$ -type transitions recorded at lower frequencies extended to  $J = 64$ . Slightly more pronounced deviations occurred at even higher  $J$  and  $K_a$ , which mainly involved the internal rotation patterns.

After each round of measurements and assignments, new spectroscopic parameters were determined. The need for additional parameters was tested by investigating the addition of one parameter at a time, searching for the one with the largest effect on reducing the weighted rms. The calculated sextic centrifugal distortion parameters were added as fixed parameters when it appeared that they may affect the lower order parameters. They were only released if this resulted in an appreciable reduction of the weighted rms, as earlier in the case of the quartic distortion parameters. In cases where two parameters provided the greatest improvement in the fit, these two parameters were added if the improvement of both parameters combined was approximately equal to the sum of improvement contributed by each parameter separately. If both parameters combined had about the same effect as one of the two, the one parameter was used that appeared to be more in line with the previous parameters. In some cases, parameters with magnitudes around five times their uncertainties or less were omitted as long as the increase in weighted rms was deemed small enough. The resulting spectroscopic parameters are given in Table 5 together with values from the B3LYP/3a quantum-chemical calculation.

## 6. Discussion

A total of 961 experimental lines were fit with 33 spectroscopic parameters to within their uncertainties on average. This corresponds to 29 lines per parameter on average. The quantum number coverage of the  $a$ -type transitions is shown in Figure 3,

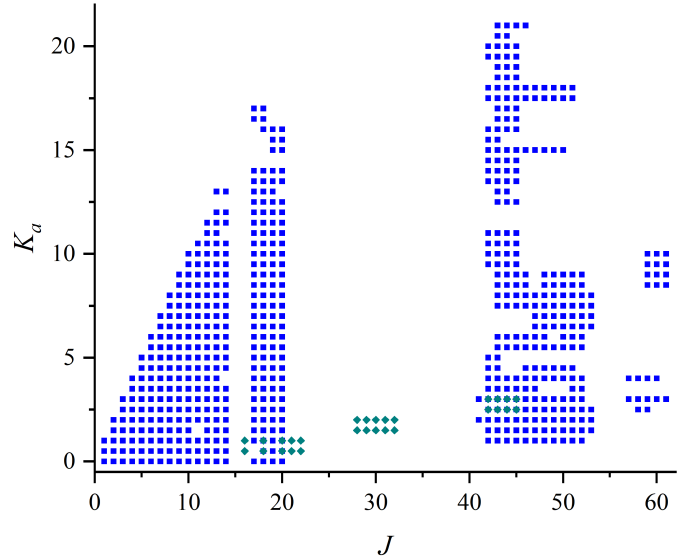


Figure 3: Quantum number coverage of the  $a$ -type transitions in the final fit. Blue squares indicate  $R$ -branch transitions and green diamonds  $Q$ -branch transitions. The  $K_a = J - K_c$  levels appear as integer values whereas the  $K_a = J - K_c + 1$  levels appear lowered by 0.5.

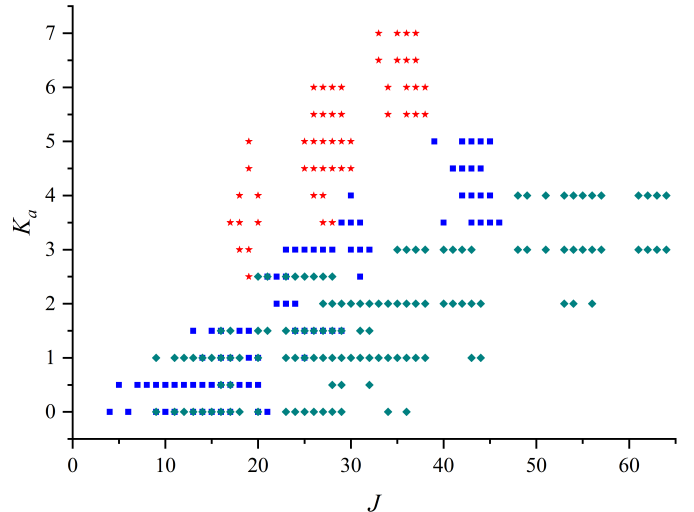


Figure 4: Same as Figure 3, but for  $b$ -type transitions. Red stars mark  $P$ -branch transitions.

Table 1: Experimental spectroscopic parameters of methylallene in comparison to values calculated at the B3LYP/3a level and previous experimental rotational and distortion parameters.

Parameter	Experimental	B3LYP/3a <sup>a</sup>	Previous [21]	Previous [22]
<i>A</i>	33997.87067 (18)	34735.5	33860. (150)	34021. (25)
<i>B</i>	4201.2822272 (99)	4181.1	4201.26 (1)	4201.301 (10)
<i>C</i>	3928.1001862 (97)	3919.5	3928.11 (1)	3928.122 (9)
$D_K \times 10^3$	1163.4093 (78)	1146.8		
$D_{JK} \times 10^3$	-55.10624 (24)	-52.42	-54.	-53.6 (2)
$D_J \times 10^3$	1.7802449 (24)	1.636	1.2	1.66 (9)
$d_1 \times 10^6$	-356.3933 (42)	-315.1		
$d_2 \times 10^6$	-8.85211 (98)	-7.096		
$H_K \times 10^6$	92.98 (11)	91.40		
$H_{KJ} \times 10^6$	-2.24855 (55)	-2.304		
$H_{JK} \times 10^9$	-152.03 (17)	-124.4		
$H_J \times 10^9$	4.6398 (23)	3.873		
$h_1 \times 10^{12}$	1830.4 (27)	1449.		
$h_2 \times 10^{12}$	158.79 (87)	117.8		
$h_3 \times 10^{12}$	15.05 (28)	10.59		
$L_{JK} \times 10^{15}$	402. (37)			
$l_1 \times 10^{15}$	-12.95 (52)			
$\rho^b$	0.165597 (32)			
$\beta^c$	5.9311 (76)			
$\epsilon$	-49.999 (13)			
$\epsilon_K \times 10^3$	22.03 (75)			
$\epsilon_J \times 10^3$	-1.773 (41)			
$\epsilon_2 \times 10^3$	-0.450 (20)			
$\epsilon_{KK} \times 10^6$	-49.1 (54)			
$\epsilon_{JK} \times 10^6$	-0.436 (89)			
$\epsilon_{JJ} \times 10^6$	0.1711 (75)			
$\epsilon_{2K} \times 10^6$	-16.45 (39)			
$\epsilon_{2J} \times 10^9$	89.0 (37)			
$\epsilon_{2KK} \times 10^9$	67.0 (43)			
$G_a \times 10^3$	-320.2 (53)			
$G_{aK} \times 10^3$	1.198 (67)			
$G_{2a} \times 10^6$	15.8 (27)			
$G_{aJK} \times 10^6$	-0.176 (11)			
$J_{\max}^b$	64			
$K_{a,\max}^b$	21			
No. transitions <sup>b</sup>	1137			
No. lines <sup>b</sup>	961			
rms	0.0119			
wrms <sup>b</sup>	0.823			

Notes: Watson's *S* reduction was utilized in the representation  $I'$ . All values in MHz units except where indicated. Numbers in parentheses are one standard deviation in units of the least significant figures. Empty fields indicate parameters not determined quantum-chemically. <sup>a</sup>Ground-state rotational and equilibrium centrifugal distortion parameters. <sup>b</sup> $\rho$ ,  $J_{\max}$ ,  $K_{a,\max}$ , the numbers of transitions and lines, and the weighted rms are dimensionless. <sup>c</sup> $\beta$  in units of degrees.

while the one for the *b*-type transitions is shown in Figure 4. The coverage of the *a*-type *R*-branch transitions reflects the frequency coverage of the present work, except that the transitions with  $J' \leq 4$  are from a previous study [21]. And even though the number of *b*-type transitions is much smaller than that of the *a*-types because of their much lower intensity, they still cover a fair fraction of the quantum number space, see Figure 4. The lower order as well as some higher order parameter were determined very well, that is with uncertainties much smaller than their magnitudes. Among the parameters with relatively large uncertainties, most are still well determined with their magnitudes being around a factor of 10 larger than their uncertainties. Two parameters,  $G_{2a}$  and  $\epsilon_{JK}$ , are not as well determined, but were retained in the fit.

The rotational and centrifugal distortion parameters agree reasonably to well with those calculated at the B3LYP/3a level. The method is computationally inexpensive and thus well suited for anharmonic calculations of a somewhat large molecule. It is quite common that calculated equilibrium distortion parameters are smaller in magnitude than the experimental ground state values, in the present case  $A_e = 34845.7$ ,  $B_e = 4201.0$ , and  $C_e = 3940.7$  MHz. However, model insufficiencies are important also as the deviations of a majority of parameters are probably larger than expected for vibrational effects alone. Model insufficiencies are most likely also responsible for the modest agreement between experimental dipole moment components,  $\mu_a = 0.397$  D and  $\mu_b = 0.071$  D [21], compared to 0.457 D and 0.054 D, respectively, from our B3LYP/3a calculation. We carried out a MP2 [34] calculation with the same triple zeta basis set later which yielded  $\mu_a = 0.400$  D and  $\mu_b = 0.076$  D, in much better agreement with the experimental values.

The Erham program determines a tunneling parameter  $\epsilon$ . Its relation to the  $\text{CH}_3$  barrier height  $V_3$  to internal rotation was investigated empirically in a study on the rotational spectrum of butynone [35]. The relation displayed some scatter, such that the conversion of one to the other needs to be viewed with some caution. Employing  $\epsilon = -50.0$  MHz (Table 5), we obtain  $V_3 \approx 513 \text{ cm}^{-1}$ , in fair agreement with  $556 \text{ cm}^{-1}$  from a previous rotational study [21]; however, this value is based on an assumption on the moment of inertia of  $\text{CH}_3$  in methylallene. On the other hand, their internal rotor splitting value  $\Delta_0 = 152.8 \pm 3$  MHz agrees well with our splitting value  $-3\epsilon = 150.0$  MHz, which is the rotationless A/E splitting.

## 7. Conclusion and outlook

We have recorded and analyzed the rotational spectrum of methylallene into the submillimeter region and obtained accurate spectroscopic parameters. The resulting calculated spectrum is accurate enough up to 720 GHz and  $J = 90$  with some restrictions concerning high values of  $K_a$ , that is  $K_a \gtrsim 20$  for *a*-type transitions and  $K_a = 12 - 11$  for *b*-type transitions. This is sufficient to search for methylallene not only in cold, dark clouds, but also in the warm parts of star-forming regions in the interstellar medium. Calculated spectra were sent to astronomers, however, no unambiguous detection has been made

to date. Deeper integrations or searches in other sources may eventually lead to its detection.

## Acknowledgement(s)

We thank the Regionales Rechenzentrum der Universität zu Köln (RRZK) for providing computing time on the DFG funded High Performance Computing System CHEOPS. Our research benefited from NASA's Astrophysics Data System (ADS).

## Disclosure statement

No potential conflict of interest was reported by the author(s).

## Data availability statement

A calculated rotational spectrum of the molecule is available in the catalog section of the CDMS [36, 2, 3] at <https://cdms.astro.uni-koeln.de/classic/entries/> as well as in the Virtual Atomic and Molecular Data Centre (VAMDC) [37] compatible version of the CDMS. Line, input, output, and other auxiliary files are available in the data section of the CDMS at <https://cdms.astro.uni-koeln.de/classic/predictions/daten/Methylallene/>. All these files have also been deposited at zenodo at <https://doi.org/10.5281/zenodo.18376494>.

## Funding

We acknowledge support by the Deutsche Forschungsgemeinschaft (DFG) via the collaborative research center SFB 1601 (project ID 500700252) subprojects A4 and Inf as well as the Gerätzentrum SCHL 341/15-1 (“Cologne Center for Terahertz Spectroscopy”). J.-C. G. is grateful for financial support by the Centre National d’Etudes Spatiales (CNES; grant number 4500065585) and by the Programme National Physique et Chimie du Milieu Interstellaire (PCMI) of CNRS/INSU with INC/INP co-funded by CEA and CNES.

## ORCID

Holger S. P. Müller <https://orcid.org/0000-0002-0183-8927>  
 Frank Lewen <https://orcid.org/0000-0003-4555-2303>  
 Jean-Claude Guillemin <https://orcid.org/0000-0002-2929-057X>  
 Stephan Schlemmer <https://orcid.org/0000-0002-1421-7281>

## References

- [1] [Https://cdms.astro.uni-koeln.de/classic/molecules](https://cdms.astro.uni-koeln.de/classic/molecules), accessed Dec. 05, 2025.
- [2] H. S. P. Müller, F. Schlöder, J. Stutzki, G. Winnewisser, The Cologne Database for Molecular Spectroscopy, CDMS: a useful tool for astronomers and spectroscopists, *J. Mol. Struct.* 742 (1-3) (2005) 215–227. doi:10.1016/j.molstruc.2005.01.027.

[3] C. P. Endres, S. Schlemmer, P. Schilke, J. Stutzki, H. S. P. Müller, The Cologne Database for Molecular Spectroscopy, CDMS, in the Virtual Atomic and Molecular Data Centre, VAMDC, *J. Mol. Spectrosc.* 327 (2016) 95–104. [arXiv:1603.03264](https://arxiv.org/abs/1603.03264), doi:10.1016/j.jms.2016.03.005.

[4] A. M. Burkhardt, K. Long Kelvin Lee, P. Bryan Changala, C. N. Shingledecker, I. R. Cooke, R. A. Loomis, H. Wei, S. B. Charnley, E. Herbst, M. C. McCarthy, B. A. McGuire, Discovery of the Pure Polycyclic Aromatic Hydrocarbon Indene (c-C<sub>9</sub>H<sub>8</sub>) with GOTHAM Observations of TMC-1, *Astrophys. J. Lett.* 913 (2) (2021) L18. [arXiv:2104.15117](https://arxiv.org/abs/2104.15117), doi:10.3847/2041-8213/abfd3a.

[5] J. Cernicharo, M. Agúndez, C. Cabezas, B. Tercero, N. Marcelino, J. R. Pardo, P. de Vicente, Pure hydrocarbon cycles in TMC-1: Discovery of ethynyl cyclopropenylidene, cyclopentadiene, and indene, *Astron. Astrophys.* 649 (2021) L15. [arXiv:2104.13991](https://arxiv.org/abs/2104.13991), doi:10.1051/0004-6361/202141156.

[6] C. Cabezas, M. Agúndez, C. Pérez, D. Villar-Castro, G. Molpeceres, D. Pérez, A. L. Steber, R. Fuentetaja, B. Tercero, N. Marcelino, A. Lesarri, P. de Vicente, J. Cernicharo, Discovery of interstellar phenalene (c-C<sub>13</sub>H<sub>10</sub>): A new piece in the chemical puzzle of PAHs in space, *Astron. Astrophys.* 701 (2025) L8. [arXiv:2508.13857](https://arxiv.org/abs/2508.13857), doi:10.1051/0004-6361/202556687.

[7] G. Wenzel, S. Gong, C. Xue, P. B. Changala, M. S. Holdren, T. H. Speak, D. A. Stewart, Z. T. P. Fried, R. H. J. Willis, E. A. Bergin, A. M. Burkhardt, A. N. Byrne, S. B. Charnley, A. Lipnicki, R. A. Loomis, C. N. Shingledecker, I. R. Cooke, M. C. McCarthy, A. J. Remijan, A. E. Wendlandt, B. A. McGuire, Discovery of the Seven-ring Polycyclic Aromatic Hydrocarbon Cyanocoronene (C<sub>24</sub>H<sub>11</sub>CN) in GOTHAM Observations of TMC-1, *Astrophys. J. Lett.* 984 (1) (2025) L36. [arXiv:2504.05232](https://arxiv.org/abs/2504.05232), doi:10.3847/2041-8213/adc911.

[8] A. N. Byrne, C. Xue, T. Van Voorhis, B. A. McGuire, Sensitivity analysis of aromatic chemistry to gas-phase kinetics in a dark molecular cloud model, *Phys. Chem. Chem. Phys.* 26 (42) (2024) 26734–26747. [arXiv:2410.09212](https://arxiv.org/abs/2410.09212), doi:10.1039/D4CP03229B.

[9] G. Esplugues, J. C. Loison, M. Agúndez, G. Molpeceres, N. Marcelino, B. Tercero, J. Cernicharo, Discovery of linear propadienone: Study of the chemistry of linear and cyclic H<sub>2</sub>C<sub>3</sub>O and H<sub>2</sub>C<sub>3</sub>S in TMC-1, *Astron. Astrophys.* In press (2026). [arXiv:2511.19775](https://arxiv.org/abs/2511.19775), doi:10.1051/0004-6361/202557355.

[10] C. N. Shingledecker, S. Álvarez-Barcia, V. H. Korn, J. Kästner, The Case of H<sub>2</sub>C<sub>3</sub>O Isomers, Revisited: Solving the Mystery of the Missing Propadienone, *Astrophys. J.* 878 (2) (2019) 80. [arXiv:1904.11396](https://arxiv.org/abs/1904.11396), doi:10.3847/1538-4357/ab1d4a.

[11] H. Niki, P. D. Maker, C. M. Savage, L. P. Breitenbach, Fourier transform ir spectroscopic observation of chlorine nitrite, ciono, formed via cl + no<sub>2</sub> (+m) → clono(+m), *Chem. Phys. Lett.* 59 (1) (1978) 78–79. doi:10.1016/0009-2614(78)85618-8. URL <https://www.sciencedirect.com/science/article/pii/0009261478856188>

[12] N. Marcelino, J. Cernicharo, M. Agúndez, E. Roueff, M. Gerin, J. Martín-Pintado, R. Mauersberger, C. Thum, Discovery of Interstellar Propylene (CH<sub>2</sub>CHCH<sub>3</sub>): Missing Links in Interstellar Gas-Phase Chemistry, *Astrophys. J. Lett.* 665 (2) (2007) L127–L130. [arXiv:0707.1308](https://arxiv.org/abs/0707.1308), doi:10.1086/521398.

[13] M. Agúndez, J. Cernicharo, M. Guélin, Discovery of interstellar ketenyl (HCCO), a surprisingly abundant radical, *Astron. Astrophys.* 577 (2015) L5. [arXiv:1504.05721](https://arxiv.org/abs/1504.05721), doi:10.1051/0004-6361/201526317.

[14] M. Fatima, H. S. P. Müller, O. Zingsheim, F. Lewen, V. M. Rivilla, I. Jiménez-Serra, J. Martín-Pintado, S. Schlemmer, Millimetre and submillimetre spectroscopy of isobutene and its detection in the molecular cloud G+0.693, *Astron. Astrophys.* 680 (2023) A25. [arXiv:2309.17236](https://arxiv.org/abs/2309.17236), doi:10.1051/0004-6361/202347112.

[15] S. Manigand, A. Coutens, J. C. Loison, V. Wakelam, H. Calcutt, H. S. P. Müller, J. K. Jørgensen, V. Taquet, S. F. Wampfler, T. L. Bourke, B. M. Kulterer, E. F. van Dishoeck, M. N. Drozdovskaya, N. F. W. Ligterink, The ALMA-PILS survey: First detection of the unsaturated 3-carbon molecules Propenal (C<sub>2</sub>H<sub>3</sub>CHO) and Propylene (C<sub>3</sub>H<sub>6</sub>) towards IRAS 16293–2422 B, *Astron. Astrophys.* 645 (2021) A53. [arXiv:2007.04000](https://arxiv.org/abs/2007.04000), doi:10.1051/0004-6361/202038113.

[16] J. Cernicharo, B. Tercero, M. Agúndez, C. Cabezas, R. Fuentetaja, N. Marcelino, P. de Vicente, CN and CCH derivatives of ethylene and ethane: Confirmation of the detection of CH<sub>3</sub>CH<sub>2</sub>CCH in TMC-1, *Astron. Astrophys.* 686 (2024) A139. [arXiv:2404.07585](https://arxiv.org/abs/2404.07585), doi:10.1051/0004-6361/202449531.

[17] J. H. Baraban, M.-A. Martin-Drumel, P. B. Changala, S. Eibenberger, M. Nava, D. Patterson, J. F. Stanton, G. B. Ellison, M. C. McCarthy, The molecular structure of gauche-1,3-butadiene: Experimental establishment of non-planarity, *Angew. Chem. Int. Ed.* 57 (7) (2018) 1821–1825. [arXiv:https://onlinelibrary.wiley.com/doi/pdf/10.1002/anie.201709966](https://arxiv.org/abs/https://onlinelibrary.wiley.com/doi/pdf/10.1002/anie.201709966), doi:10.1002/anie.201709966. URL <https://onlinelibrary.wiley.com/doi/abs/10.1002/anie.201709966>

[18] J. Saltiel, D. F. Sears, A. M. Turek, Uv spectrum of the high energy conformer of 1,3-butadiene in the gas phase, *J. Phys. Chem. A* 105 (32) (2001) 7569–7578. [arXiv:https://doi.org/10.1021/jp011493c](https://arxiv.org/abs/https://doi.org/10.1021/jp011493c), doi:

10.1021/jp011493c.

URL <https://doi.org/10.1021/jp011493c>

[19] M. Agúndez, C. Cabezas, N. Marcelino, B. Tercero, R. Fuentetaja, P. de Vicente, J. Cernicharo, A search for the three isomers of cyano-1,3-butadiene in TMC-1: Implications for bottom-up routes involving 1,3-butadiene, *Astron. Astrophys.* 697 (2025) A82. arXiv:2503.23841, doi:10.1051/0004-6361/202554343.

[20] J. Cernicharo, C. Cabezas, M. Agúndez, B. Tercero, N. Marcelino, J. R. Pardo, F. Tercero, J. D. Gallego, J. A. López-Pérez, P. de Vicente, Discovery of allenyl acetylene,  $H_2CCCHCCH$ , in TMC-1. A study of the isomers of  $C_5H_4$ , *Astron. Astrophys.* 647 (2021) L3. arXiv:2103.01125, doi:10.1051/0004-6361/202140482.

[21] D. R. Lide, Jr., D. E. Mann, Microwave Spectra of Molecules Exhibiting Internal Rotation. II. Methylallene, *J. Chem. Phys.* 27 (4) (1957) 874–877. doi:10.1063/1.1743868.

[22] T. Ogata, Microwave-spectra and substitution structure of methylallene, *J. Phys. Chem.* 96 (5) (1992) 2089–2091. doi:10.1021/j100184a014.

[23] C. D. Hurd, R. N. Meinert, Synthesis and pyrolysis of methylallene and ethylacetylene, *J. Am. Chem. Soc.* 53 (1) (1931) 289–300. doi:10.1021/ja01352a040. URL <https://doi.org/10.1021/ja01352a040>

[24] M. H. Ordu, H. S. P. Müller, A. Walters, M. Nuñez, F. Lewen, A. Belloche, K. M. Menten, S. Schlemmer, The quest for complex molecules in space: laboratory spectroscopy of n-butyl cyanide, n-C<sub>4</sub>H<sub>9</sub>CN, in the millimeter wave region and its astronomical search in Sagittarius B2(N), *Astron. Astrophys.* 541 (2012) A121. arXiv:1204.2686, doi:10.1051/0004-6361/201118738.

[25] M. A. Martin-Drumel, J. van Wijngaarden, O. Zingsheim, F. Lewen, M. E. Harding, S. Schlemmer, S. Thorwirth, Millimeter- and submillimeter-wave spectroscopy of disulfur dioxide, OSSO, *J. Mol. Spectrosc.* 307 (2015) 33–39. doi:10.1016/j.jms.2014.11.007.

[26] M. J. Frisch, G. W. Trucks, H. B. Schlegel, G. E. Scuseria, M. A. Robb, J. R. Cheeseman, G. Scalmani, V. Barone, G. A. Petersson, et al., Gaussian 16, Revision C.01, Gaussian, Inc., Wallingford CT (2019).

[27] A. D. Becke, Density-functional thermochemistry. III. The role of exact exchange, *J. Chem. Phys.* 98 (7) (1993) 5648–5652. doi:10.1063/1.464913.

[28] C. Lee, W. Yang, R. G. Parr, Development of the Colle-Salvetti correlation-energy formula into a functional of the electron density, *Phys. Rev. B* 37 (2) (1988) 785–789. doi:10.1103/PhysRevB.37.785.

[29] T. H. Dunning, Jr., Gaussian basis sets for use in correlated molecular calculations. I. The atoms boron through neon and hydrogen, *J. Chem. Phys.* 90 (2) (1989) 1007–1023. doi:10.1063/1.456153.

[30] K. Tanaka, T. Tanaka, I. Suzuki, Dipole moment function of carbonyl sulfide from analysis of precise dipole moments and infrared intensities, *J. Chem. Phys.* 82 (7) (1985) 2835–2844. doi:10.1063/1.448285.

[31] J. G. Lahaye, R. Vandenhaute, A. Fayt, CO<sub>2</sub> laser saturation Stark spectra and global Stark analysis of carbonyl sulfide, *J. Mol. Spectrosc.* 119 (2) (1986) 267–279. doi:10.1016/0022-2852(86)90023-8.

[32] P. Groner, Effective rotational Hamiltonian for molecules with two periodic large-amplitude motions, *J. Chem. Phys.* 107 (12) (1997) 4483–4498. doi:10.1063/1.474810.

[33] P. Groner, Effective rotational Hamiltonian for molecules with internal rotors: Principles, theory, applications and experiences, *J. Mol. Spectrosc.* 278 (2012) 52–67. doi:10.1016/j.jms.2012.06.006.

[34] C. Møller, M. S. Plesset, Note on an Approximation Treatment for Many-Electron Systems, *Phys. Rev.* 46 (7) (1934) 618–622. doi:10.1103/PhysRev.46.618.

[35] K. G. Lengsfeld, P. Buschmann, F. Dohrmann, J.-U. Grabow, A prochiral precursor in space? Accurate laboratory characterization of acetylacetylene in the cm-wave region, *J. Mol. Spectrosc.* 377 (2021) 111441. doi:10.1016/j.jms.2021.111441.

[36] H. S. P. Müller, S. Thorwirth, D. A. Roth, G. Winniwer, The Cologne Database for Molecular Spectroscopy, CDMS, *Astron. Astrophys.* 370 (2001) L49–L52. doi:10.1051/0004-6361:20010367.

[37] D. Albert, B. K. Antony, Y. A. Ba, Y. L. Babikov, P. Bolland, V. Boudon, F. Delahaye, G. Del Zanna, M. S. Dimitrijević, B. J. Drouin, M.-L. Dubernet, F. Duensing, M. Emoto, C. P. Endres, A. Z. Fazliev, J.-M. Glorian, I. E. Gordon, P. Gratier, C. Hill, D. Jevremović, C. Joblin, D.-H. Kwon, R. V. Kochanov, E. Krishnakumar, G. Leto, P. A. Loboda, A. A. Lukashevskaya, O. M. Lyulin, B. P. Marinković, A. Markwick, T. Marquart, N. J. Mason, C. Mendoza, T. J. Millar, N. Moreau, S. V. Morozov, T. Möller, H. S. P. Müller, G. Mulas, I. Murakami, Y. Pakhomov, P. Palmeri, J. Penguen, V. I. Perevalov, N. Piskunov, J. Postler, A. I. Privezentsev, P. Quinet, Y. Ralchenko, Y.-J. Rhee, C. Richard, G. Rixon, L. S. Rothman, E. Roueff, T. Ryabchikova, S. Sahal-Bréchot, P. Scheier, P. Schilke, S. Schlemmer, K. W. Smith, B. Schmitt, I. Y. Skobelev, V. A. Srecković, E. Stempels, S. A. Tashkun, J. Tennyson, V. G. Tyuterev, C. Vastel, V. Vujčić, V. Wakelam, N. A. Walton, C. Zeippen, C. M. Zwölf, A Decade with VAMDC: Results and Ambitions, *Atoms* 8 (4) (2020) 76. doi:10.3390/atoms8040076.